

Matching the Bare and \overline{MS} Charm Quark Masses Using Weak Coupling Simulations

I. F. Allison^{*a} †, K. Y. Wong^b, C. T. H. Davies^b, C. McNeile^b, H. D. Trottier^c, E. Dalgic^c,
J. Wu^a, E. Follana^d, R. R. Horgan^e, G. P. Lepage^f, J. Shigemitsu^g,
for the HPQCD collaboration

^a TRIUMF, 4004 Wesbrook Mall, Vancouver, BC, V6T 2A3, Canada

^b Department of Physics and Astronomy, University of Glasgow, Glasgow, G12 8QQ, UK

^c Department of Physics, Simon Fraser University, Vancouver, BC, V5A 1S6, Canada

^d Department of Theoretical Physics, University of Zaragoza, E-50009, Zaragoza, Spain,

^e DAMTP, CMS, University of Cambridge, Cambridge, CB3 0WQ, UK

^f Laboratory for Elementary-Particle Physics, Cornell University, Ithaca, NY, 14853, USA

^g Physics Department, The Ohio State University, Columbus, Ohio, 43210, USA

We provide a new determination of the charm quark mass using the Highly Improved Staggered Quark (HISQ) action, finding $m_c^{\overline{MS}}(3\text{ GeV}) = 0.983(23)\text{ GeV}$. Our determination makes extensive use of second order lattice perturbation theory in matching the bare lattice mass to the \overline{MS} scheme. This matching utilises both traditional diagrammatic perturbation theory and weak coupling simulations. The second of these techniques allows us to extract perturbative coefficients from Monte-Carlo simulations and the process of doing this is laid out in some detail here.

The XXVI International Symposium on Lattice Field Theory

July 14-19 2008

Williamsburg, Virginia, USA

^{*}Speaker.

[†]Email:iana@triumf.ca

1. Introduction

The quark masses are important both as fundamental parameters and, more pragmatically, as inputs to experimental determinations of CKM matrix elements [1]. The charm quark is particularly important because of the large flavour physics program, but it has been somewhat neglected on the lattice due to the difficulty in simulating it accurately. In these proceedings, we make use of the highly-improved staggered quark (HISQ) action [2] to extract a value for the charm quark mass from dynamical lattice QCD. Empirically, the HISQ action is known to reduce the $\mathcal{O}(\alpha_s a^2)$ errors which remain in the AsqTad action, and which are thought to be taste-changing errors, making precision charm physics possible [2]. It does this by repeating the AsqTad link smearing, which further suppresses taste changing interactions, and also by correcting the dispersion relation through adjustment of the N aik term coefficient. In this work, we aim to use these features to calculate the charm quark mass from η_c correlators on the lattice.

In quoting a determination of a quantity such as the charm quark mass, it is customary to convert to the \overline{MS} renormalization scheme and to use a standard scale (e.g. 3 GeV). To do this directly from a determination of the bare lattice QCD mass requires lattice perturbation theory. The trend towards increasingly complicated actions, such as HISQ, has made most calculations of this type a major computational undertaking. One tool developed in response to this is the use of weak coupling or *high- β* simulations [3]. At sufficiently large values of the coupling β (equivalently, sufficiently small lattice spacings) a lattice simulation will have a small physical volume and a very large cutoff ($\approx \pi/a$). These are precisely the conditions required to probe the perturbative regime of QCD and when perturbation theory is done in this way (by Monte-Carlo) all orders are automatically included. When it is used in combination with a technique like constrained curve fitting, the high- β technique can allow diagrammatic results to be extended to the next order at the cost of running some extra simulations, provided the quality of the high- β results is sufficient. This approach has been successfully demonstrated in [4]. Of course, there are some complications, mostly related to the very small volumes of the simulations, but the two most significant problems: the existence of zero modes and \mathbb{Z}_3 tunneling, are known to be effectively resolved by the use of (color) twisted boundary conditions[5], see e.g. [6]. In this work, we will use high- β simulations with twisted boundary conditions on all of the spatial dimensions to do part of the second order matching.

The recently published determination of [7] also used HISQ quarks and a mixture of continuum and lattice techniques to calculate the charm quark mass, finding $m_{\overline{MS}}(3 \text{ GeV}) = 0.986(10) \text{ GeV}$. The calculation we will present uses a completely different method, extracting m_c from η_c correlators before manually matching to the \overline{MS} scheme. Together we view these independent calculations as giving important cross checks of one another.

2. Matching to the \overline{MS} Scheme

The lattice charm quark mass am_c can be matched to the \overline{MS} scheme mass $m_{\overline{MS}}$ using the on-shell mass M as an intermediate stage.

$$\begin{aligned} m_{\overline{MS}}(\mu) &= M \left[1 + (B_{11}l + B_{10}) \alpha_{\overline{MS}}(\mu) + (B_{22}l^2 + B_{21}l + B_{20}) \alpha_{\overline{MS}}^2(\mu) \right] + \mathcal{O}(\alpha_{\overline{MS}}^3) \\ M &= am_c \left[1 + (A_{11}L + A_{10}) \alpha_L + (A_{22}L^2 + A_{21}L + A_{20}) \alpha_L^2 \right] + \mathcal{O}(\alpha_L^3), \end{aligned} \quad (2.1)$$

where $L = \log am_c$ and $l = \log \mu/M$. The relation between $m_{\overline{MS}}$ and M (the B coefficients) is given to third order in [8] so only the A coefficients are unknown. The connections between $\alpha_L \rightarrow \alpha_V$, and $\alpha_{\overline{MS}} \rightarrow \alpha_V$ are given in [9] and [10] respectively. Writing $m_{\overline{MS}}$ in terms of am_c to second order in α_V and demanding that the unphysical dependence on $L = \log am_c$ vanishes gives conditions on the coefficients A_{11}, A_{22} and A_{21} which result in the form

$$\begin{aligned} m_{\overline{MS}}(\mu) &= am_c \left(1 + (Z_{11}l_{a\mu} + Z_{10}) \alpha_V(aq^*) + (Z_{22}l_{a\mu}^2 + Z_{21}l_{a\mu} + Z_{20}) \alpha_V^2(aq^*) \right) + \mathcal{O}(\alpha_V^3) \\ &= am_c + c_1(m_q a) \alpha_V(aq^*) + (c_{2,q} + c_{2,g}) \alpha_V^2(aq^*) + \mathcal{O}(\alpha_V^3), \end{aligned} \quad (2.2)$$

with $l_{a\mu} = \log a\mu$ and

$$\begin{aligned} Z_{11} &= -\frac{2}{\pi}, & Z_{10} &= A_{10} - \frac{4}{3\pi}, & Z_{22} &= \frac{15}{2\pi^2} - \frac{n_f}{3\pi^2}, \\ Z_{21} &= \left(\frac{2 \log aq}{3\pi^2} - \frac{5}{18\pi^2} \right) n_f - \frac{11 \log aq}{\pi^2} - \frac{7}{12\pi^2} - \frac{2A_{10}}{\pi}, \\ Z_{20} &= \left(\frac{\log \pi/aq}{3\pi} A_{10} + \frac{4 \log aq}{9\pi^2} + \frac{53}{432\pi^2} + \frac{1}{18} \right) n_f + A_{20} \\ &\quad + \left(\frac{2}{3\pi} - \frac{11 \log \pi/aq}{2\pi} - v_{1,0} \right) A_{10} + \frac{\zeta_3}{6\pi^2} - \frac{2 + \log 2}{9} - \frac{22 \log aq}{3\pi^2} - \frac{257}{32\pi^2}. \end{aligned} \quad (2.3)$$

The splitting of the fermionic and gluonic portions of c_2 in the second line of equation (2.2) is motivated by there being only 4 fermionic diagrams for the second order mass renormalization. These diagrams have been evaluated using diagrammatic perturbation theory (see [11] for an outline of this calculation, final results are in preparation). The remaining diagrams which contribute to $c_{2,g}$ represent a much larger undertaking and are our motivation for the use of the high- β technique. One advantage of the split is that we only require *quenched* results for $c_{2,g}$. The remaining unknown coefficients A_{10} and $A_{20} = A_{20,g} + A_{20,f}$, can then be expressed in the following way

$$A_{10} = \frac{c_1}{am_c} + \frac{2}{\pi} L, \quad (2.4)$$

$$\begin{aligned} A_{20,g} &= \left(\frac{L^2}{3\pi^2} - \frac{1 + 4 \log \pi}{6\pi^2} L - \frac{c_1 \log \pi/aq}{3\pi am_c} \right) n_f - \frac{7}{2\pi^2} L^2 + \\ &\quad + \left(\frac{2c_1}{\pi} + \frac{79 + 132 \log \pi + 24\pi v_{1,0}}{12\pi^2} \right) L + \frac{2\pi c_{2,g} + 11c_1 \log \pi/aq + 2\pi c_1 v_{1,0}}{2am_c}. \end{aligned} \quad (2.5)$$

$A_{20,f}$ comes from the diagrammatic analysis of [11]. Together with equation (2.3) these coefficients allows us to evaluate equation (2.2) and extract a physical values of $m_{\overline{MS}}$.

3. Results

3.1 The Lattice Charm Quark Mass

The lattice bare charm quark mass was tuned by adjusting it until the η_c mass agreed with experiment on four ensembles of the MILC collaboration's configurations [12]. In this tuning the scale was set using MILC values of r_1/a and the value $r_1 = 0.321(5)$ fm [13]. The bare mass was adjusted for any mistuning (a very small effect in all cases) and then converted to the bare tree level

mass¹ which is the quantity related to the \overline{MS} mass in equation (2.2). The $m_{c,tree}$ values are given in Table 1.

Size	$u_0 am_l$	$u_0 am_s$	am_c	am_{η_c}	$m_{c,tree}/\text{GeV}$	$1 + \varepsilon$	r_1/a
$16^3 \times 48$	0.0194	0.0484	0.85	2.26964(17)	1.100(2)(2)	0.66	2.129(11)
	0.0097	0.0484	0.85	2.27031(16)	1.098(0)(2)	0.66	2.133(11)
$20^3 \times 64$	0.02	0.05	0.648	1.84153(17)	1.040(5)(1)	0.79	2.650(8)
	0.01	0.05	0.66	1.87142(12)	1.041(6)(2)	0.79	2.610(12)
$24^3 \times 64$	0.005	0.05	0.65	1.84949(11)	1.039(3)(2)	0.79	2.632(13)
$28^3 \times 96$	0.0124	0.031	0.427	1.30731(11)	0.9718(5)(11)	0.885	3.711(13)
	0.0062	0.031	0.43	1.31693(12)	0.9715(5)(11)	0.885	3.684(12)
$48^3 \times 144$	0.0036	0.018	0.28	0.91555(8)	0.9129(25)(9)	0.949	5.277(16)

Table 1: Simulation parameters for extracting the lattice charm quark mass. The value of the correction of the naïk term, ε used here was determined non-perturbatively forcing the “speed of light” to be 1. This differs, but not significantly, from the series definition of ε used in the perturbative portion of our calculations. The value of r_1 , used to set the scale, was taken to be $r_1 = 0.321(5)$ fm

3.2 High- β Perturbative Results

	HISQ	ASQTAD
$L^3 \times T$	$6^3 \times 16, 8^3 \times 20, 10^3 \times, 12^3 \times 20$	$6^3 \times 16, 8^3 \times 20, 10^3 \times, 12^3 \times 20$
β	15, 16, 20, 24, 32, 46, 62, 70, 92	15, 16, 20, 24, 32, 46, 62, 70, 92
m_0	0.30, 0.43, 0.50, 0.66, 0.85	0.30, 0.40, 0.50, 0.60, 0.70

Table 2: Parameters for the high- β simulations.

We performed high- β simulations for valence HISQ and AsqTad quarks at the parameters given in table 2. To extract c_1 and $c_{2,g}$ we started from the on shell mass $M(L, \beta)$ determined by simulating quark propagators in a Coulomb+Axial gauge², and then fitting to the form

$$aM_{pole} = E_1 + c_1 \alpha_V(aq^*) + c_{2,g} \alpha_V^2(aq^*) + \dots \quad (3.1)$$

Because high- β results are essentially perturbations around the free field, we used constrained curve fitting with the first term set to the free field energy of the HISQ action, allowing us to evaluate finite volume values for c_1 and $c_{2,g}$. The values of $\alpha_V(aq^*)$ were evaluated for each simulation by measuring the plaquette and using the three loop expansion of $\log_{W_{1 \times 1}}$ given in [4] to extract $\alpha_V(q_{plaq}^*)$ which was then evolved to the q^* relevant to our simulations.

3.3 Comparison of HISQ c_1 with Diagrammatic Perturbation Theory

Fits to equation (3.1) were performed including terms up to $\mathcal{O}(\alpha_V^4)$ with priors of 0 ± 5 for all of the c_i . We used the resulting c_1 values as a check on our method by comparing to the corresponding

¹The tree level mass is related to the bare mass via $m_{tree} = m_0 \left(1 - \frac{3}{80} m_0^4 + \frac{23}{2240} m_0^6 + \frac{1783}{573600} m_0^8 - \frac{76943}{23654400} m_0^{10} + \mathcal{O}(m_0^{12}) \right)$ for HISQ. This relation can be determined from the free field HISQ action.

²This is not the traditional maximal-tree gauge but is modified to take account of the twisted boundary conditions.

finite volume diagrammatic perturbation theory values as shown in figure 1. Our results were then extrapolated to the infinite volume limit, where we included terms up to fourth order in the fits with priors of 0 ± 3 for all parameters. These results were also compared to diagrammatic perturbation theory results and are again shown in figure 1.

$$c_1(L) = c_1(L = \infty) + \frac{X_{c,1}}{L} + \frac{X_{c,2}}{L^2} + \dots$$

mass	c_1^{MC}	c_1^{PT}
0.30	0.4477(17)	0.4505(7)
0.43	0.4932(12)	0.4921(7)
0.66	0.5979(15)	0.5978(7)
0.85	0.6634(15)	0.6693(7)

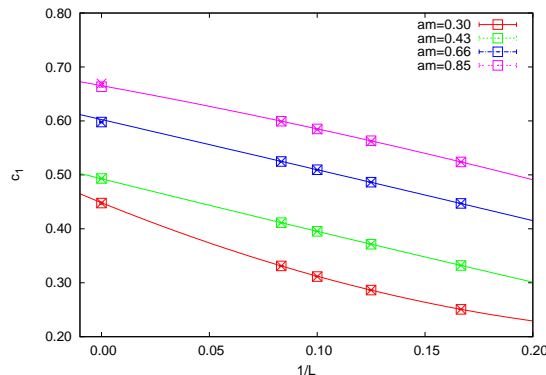


Figure 1: c_1 infinite volume extrapolations. Boxes are high- β results, crosses are diagrammatic PT results. The errors come from bootstrapping the entire analysis with 1000 bootstrap re-samples.

3.4 Comparison of AsqTad $c_{2,g}$ with Diagrammatic Perturbation Theory

For AsqTad valence quarks, c_1 and $c_{2,g}$ have already been calculated using diagrammatic perturbation theory in [14]. We used finite volume values of c_1 as priors to aid our extraction of $c_{2,g}$ and then extrapolated to the infinite volume limit via³

$$c_{2,g}(L) = c_{2,g}(L = \infty) + \frac{1}{L}(X_{c_{2,1}} + Y_{c_{2,1}} \log L^2) + \frac{1}{L^2}(X_{c_{2,2}} + Y_{c_{2,2}} \log L^2) + \dots \quad (3.2)$$

where $Y_{c_{2,1}} = \frac{11}{4\pi} X_{c_{1,1}}$ and $X_{c_{1,1}}$ is the same quantity which appears in extrapolation of c_1 and which we were able to use as a further constraint in our fits. The results of these fits are given in figure 2 and we interpret them as lending weight to our $c_{2,g}$ calculation for HISQ.

4. HISQ $c_{2,g}$ From High- β

The new result which we present here is a determination of the gluonic part of the c_2 coefficient for HISQ, for which there are no corresponding diagrammatic perturbation theory results. Again we constrained the finite volume c_1 coefficients with diagrammatic results and $X_{c_{1,1}}$ from our c_1 fits. The final results are shown in figure 3. The results are encouraging with the possible exception of the result for $am = 0.30$ which may be affected by finite volume corrections. We are currently investigating this possibility by running at larger volumes.

5. Conclusions

The high- β method has allowed us to extract a second order perturbative coefficient which would otherwise have been a *very* expensive calculation in diagrammatic perturbation theory. To-

³The justification for this form for the extrapolation comes from [6].

mass	$c_{2,g}^{MC}$	$c_{2,g}^{PT}$
0.30	1.182(94)	1.00(2)
0.40	1.350(99)	1.22(3)
0.60	1.72(11)	1.65(3)
0.70	2.02(13)	2.12(4)

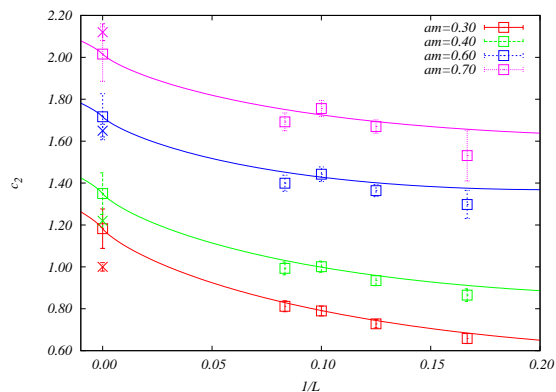


Figure 2: AsqTad $c_{2,g}$ infinite volume extrapolations. The boxes are our high- β results and the corresponding infinite volume extrapolation. The crosses are diagrammatic perturbation theory results. For this check, the analysis was *not* bootstrapped, errors are fitting/statistical only.

mass	$c_{2,g}$
0.30	0.327(34)
0.43	0.515(38)
0.66	0.130(56)
0.85	-0.438(63)

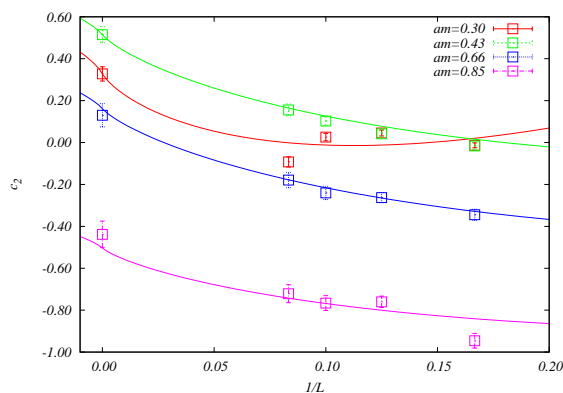


Figure 3: $c_{2,g}$ Infinite volume extrapolation for HISQ. The curved lines in the plot are fits to equation 3.3. The errors come from bootstrapping the analysis with 1000 bootstrap re-samples.

gether with calculations of c_1 , $c_{2,q}$ and equation (2.2) this allows us to provide a two loop determination of the charm quark mass using HISQ valence quarks. The final result for each lattice spacing we used is given in figure 4. The quoted continuum value comes from fitting all lattice spacings simultaneously while demanding a single common charm quark mass, allowing for higher order perturbative and discretization errors.

Beyond statistical/fitting errors, the other important sources of error are the orders excluded in the perturbative matching and the overall scale determination. We estimated the error from the perturbative matching by repeating our analysis but including the third order perturbative coefficients with A_{30} floated as a very wide prior (0 ± 45). The resulting determinations are also shown in figure 4 and suggest that estimating missing order terms by twice a typical value of $\alpha_V^3 \approx 0.22^3$ used in the matching is conservative. The error from setting the overall scale (which we do via r_1) was estimated as 0.5% from an overall error of 1.5% on r_1 because the r_1 error affects only the binding energy for the η_c (see [7]). Including these sources of error, our preliminary result is

$$m_c^{\overline{MS}}(\mu = 3 \text{ GeV}) = 0.9830(64)(49)(213) \text{ GeV} \quad (\text{stat./fitting})(\text{scale})(\text{higher orders}). \quad (5.1)$$

A more systematic determination, including better estimates of the effect of missing higher order

	mass	$m_c^{\overline{MS}}(3\text{ GeV})$
v.coarse	0.28	0.9729(53)
coarse	0.43	0.9777(12)
fine	0.66	0.9745(59)
s.fine	0.85	0.9774(18)
continuum	—	0.9830(64)

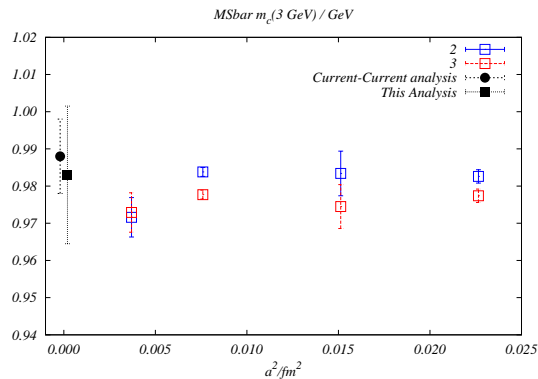


Figure 4: Blue points come from full second order analysis, red points come from fits which include a parametrization of the third order terms. The black circle comes from the analysis of [7].

matching and chiral effects is ongoing and will appear subsequently. At present though, our preliminary result is in very good agreement with the determination of [7] though with a slightly larger error. We interpret this result as a striking demonstration of the capabilities of modern lattice simulations using highly improved actions such as HISQ to give precise and physically relevant results needed by the rest of the particle physics community.

References

- [1] V. Ahrens, T. Becher, M. Neubert and L. L. Yang, arXiv:0808.3008 [hep-ph].
- [2] E. Follana *et al.* [HPQCD Collaboration and UKQCD Collaboration], Phys. Rev. D **75**, 054502 (2007) [arXiv:hep-lat/0610092].
- [3] W. Dimm, G. P. Lepage and P. B. Mackenzie, Nucl. Phys. Proc. Suppl. **42**, 403 (1995) [arXiv:hep-lat/9412100].
- [4] K. Y. Wong, H. D. Trottier and R. M. Woloshyn, Phys. Rev. D **73**, 094512 (2006) [arXiv:hep-lat/0512012].
- [5] M. Luscher and P. Weisz, Nucl. Phys. B **266**, 309 (1986).
- [6] H. D. Trottier, N. H. Shakespeare, G. P. Lepage and P. B. Mackenzie, Phys. Rev. D **65**, 094502 (2002) [arXiv:hep-lat/0111028].
- [7] I. Allison *et al.*, Phys. Rev. D **78**, 054513 (2008) arXiv:0805.2999 [hep-lat].
- [8] K. G. Chetyrkin and M. Steinhauser, Nucl. Phys. Proc. Suppl. **89**, 58 (2000).
- [9] H. D. Trottier, Nucl. Phys. Proc. Suppl. **129**, 142 (2004) [arXiv:hep-lat/0310044].
- [10] Y. Schroder, Phys. Lett. B **447**, 321 (1999) [arXiv:hep-ph/9812205].
- [11] E. Dalgic *et al.*, PoS **LAT2007**, 239 (2007).
- [12] C. W. Bernard *et al.*, Phys. Rev. D **64**, 054506 (2001) [arXiv:hep-lat/0104002].
- [13] A. Gray, I. Allison, C. T. H. Davies, E. Dalgic, G. P. Lepage, J. Shigemitsu and M. Wingate, Phys. Rev. D **72**, 094507 (2005) [arXiv:hep-lat/0507013].
- [14] Q. Mason, H. D. Trottier, R. Horgan, C. T. H. Davies and G. P. Lepage [HPQCD Collaboration], Phys. Rev. D **73**, 114501 (2006) [arXiv:hep-ph/0511160].